6561

Interaction of the Fusion Inhibiting Peptide Carbobenzoxy-D-Phe-L-Phe-Gly with N-Methyldioleoylphosphatidylethanolamine Lipid Bilayers

K. V. Damodaran and Kenneth M. Merz, Jr.*

*Contribution from the Department of Chemistry, 152 Davey Laboratory,
The Pennsylvania State University, University Park, Pennsylvania 16802*

Received February 3, 1995[®]

Abstract: We present the results of a molecular dynamics simulation of the fusion inhibiting peptide carbobenzoxy-D-Phe-L-Phe-Gly interacting with N-methyldioleoylphosphatidylethanolamine (N-Me-DOPE) bilayers. Simulations have been carried out with the peptide C-terminus both in the neutral and negatively charged states. It appears that the insertion of the phenylalanyl side chains into the lipid hydrocarbon region causes a significant increase in the order parameters near the carbonyl region and a decrease in the water penetration in the head group region, rendering this region gel-like. The negatively charged C-termini helps to anchor the peptides at the bilayer-water interface and this enhances the ordering capability of the peptide. We suggest that the increase in lipid ordering could be the molecular mechanism for the observed fusion inhibition.

Introduction

Membrane fusion is an important step in many biological processes such as endocytocis, fertilization, and infection of host cells by enveloped viruses.[1-6] The delivery of viral nucleocapsid into the host cell is activated either by viral fusion to the plasma membrane at neutral pH or fusion to the endosomal membrane at the slightly acidic pH of the cytoplasm. The initial attachment of the virus to the target membrane and subsequent fusion are facilitated by spike glycoproteins in the outer membrane of the virus, which undergo irreversible conformational changes, exposing the binding and fusion regions to the target cell. Specific examples are the F glycoprotein of the sendai virus, hemagglutinin (HA) of influenza virus, or gp120/41 of the human immunodeficiency virus (HIV).[7-9] In the case of hemagglutinin, for example there are two subunits (HA$_1$ and HA$_2$) in which HA$_1$ is the binding site and HA$_2$ is responsible for the fusion activity.[2,10] The "fusion peptide" which is thought

to interact with the target cell membrane is a highly hydrophobic region located at the N-terminus of the HA$_2$ and has been found to be highly conserved in different systems.[2,9]

Structural characteristics of the lipids involved have been shown to have an important role in fusion reactions, particularly in model systems.[10] In a fusion event the membranes involved have to overcome the repulsion due to the so called hydration forces and also electrostatic forces, in the case of charged bilayers.[11] The intervening water molecules have to be removed before the formation of fusion intermediates, which are thought to be nonbilayer structures.[12] Thus the conditions under which fusion occurs are also related to the phase properties of the lipids in the bilayers. For example, fusion activity has been observed in neat N-methyldioleoylphosphatidylethanolamine (N-Me-DOPE) and N-Me-DOPE/DOPC bilayers in a temperature range below the lamellar to inverted hexagonal (H$_{II}$) phase transition temperature (T_H). This is verified by the presence of an isotropic ^{31}P resonance which indicates the formation of nonbilayer phases.[12,13]

It has been observed that small peptides with sequence similar to the N-terminal regions of fusion peptides are capable of inhibiting virus-cell fusion. Particular examples are Z-D-Phe-L-Phe-Gly (ZfFG) and Z-L-Phe-L-Tyr investigated by Richardson and co-workers.[14,15] Early investigations by these workers[15] suggested the existence of specific binding sites on the cell membrane for which both the viral fusion peptides and the fusion inhibiting peptides (FIP) compete, thus resulting in the fusion inhibition. However, more recent studies by Kelsey *et*

® Abstract published in *Advance ACS Abstracts,* June 1, 1995.

(1) Burger, K. N. J.; Verkleij, A. J. Membrane Fusion. *Experientia* **1990,** *46,* 631–644.

(2) White, J. M. Membrane Fusion. *Science* **1992,** *258,* 917–924.

(3) Blobel, C. P.; Wolfsberg, T. G.; Turck, C. W.; Myles, D. G.; Primakoff, P.; White, J. M. A Potential Fusion Peptide and an Integrin Ligand Domain in a Protein Active in Sperm-Egg Fusion. *Nature* **1992,** *356,* 248–252.

(4) Muga, A.; Neugebauer, W.; Hirama, T.; Surewicz, W. K. Membrane Interaction and Conformational Properties of the Putative Fusion Peptide of PH-30, a Protein Active in Sperm-Egg Fusion. *Biochemistry* **1994,** *33,* 4444–4448.

(5) Hoekstra, D. J. Membrane Fusion of Enveloped Viruses: Especially a Matter of Proteins. *Bioener. Biomem.* **1990,** *22,* 121–155.

(6) *Viral Fusion Mechanisms*; Bentz, J., Ed.; CRC Press: Boca Raton, FL, 1993, pp 529.

(7) Nieva, L.; Nir, S.; Muga, A.; Goni, F. M.; Wilschut, J. Interaction of the HIV-1 Fusion Peptide with Phospholipid Vesicles: Different Structural Requirements for Fusion and Leakage. *Biochemistry* **1994,** *33,* 3201–3209.

(8) Ellens, H.; Larsen, C. In CD4-Induced Change in gp120/41 Conformation and its Potential Relationship to Fusion. *Viral Fusion Mechanisms*; Bentz, J., Ed.; CRC Press: Boca Raton, FL, 1993; pp 291–312.

(9) Gallaher, W. R. Detection of a Fusion Peptide Sequence in the Transmembrane Protein of Human Immunodeficiency Virus. *Cell* **1987,** *50,* 327–328.

(10) Bentz, J.; Alford, D.; Ellens, H. Liposomes, Membrane Fusion and Cytoplasmic Delivery. In *The Structure of Biological Membranes*; Yeagle, P. L., Ed.; CRC Press: Boca Raton, FL, 1992; pp 915–947.

(11) Gennis, R. B. *Biomembranes: Molecular Structure and Function*; Springer-Verlag: New York, 1989.

(12) Ellens, H.; Seigel, D. P.; Alford, D.; Yeagle, P. L.; Boni, L.; Lis, L. J.; J., Q. P.; Bentz, J. Membrane Fusion and Inverted Phases. *Biochemistry* **1989,** *28,* 3692–3703.

(13) Ellens, H.; Bentz, J.; Szoka, F. C. Fusion of Phosphatidylethanolamine-Containing Liposomes and Mechanism of the L$_α$–H$_{II}$ Phase Transition. *Biochemistry* **1986,** *25,* 4141–4147.

(14) Richardson, C. D.; Scheid, A.; Choppin, P. W. Specific Inhibition of Paramyxovirus and Myxovirus Replication by Oligopeptides with Amino Acid Sequences Similar to Those at the N-Termini of the F$_1$ or AH$_2$ Viral Polupeptides. *Virology* **1980,** *105,* 205.

(15) Richardson, C. D.; Choppin, P. W. Oligopeptides That Specifically Inhibit Membrane Fusion by Paramyxoviruses: Studies on the Site of Action. *Virology* **1983,** *131,* 518–532.

al. have shown that these peptides are also capable of inhibiting vesicle–vesicle and vesicle–virus fusion involving large unilamellar vesicles of *N*-methyldioleoylphosphatidylethanolamine (DOPE-Me), which suggests that the peptide–membrane interaction is nonspecific.[16,17] Their investigations also showed that these peptides inhibit the formation of highly curved phospholipid structures similar to those found in the H_{II} phase which are hypothesized to be related to the intermediate structures formed along the fusion pathway.[18] Epand *et al.* have also shown that the blocking carbobenzoxy group at the N-terminus and the partial negative charge on these peptides are crucial for the fusion inhibiting activity.[19] In particular, their experiments showed that by having an unblocked N-terminus (which could be neutral or charged) and a blocked C-terminus these peptides could act as "fusion peptides" enhancing non-bilayer phase formation and membrane leakage, rather than inhibiting these events. Following Epand *et al.*, we refer to this modified peptide (D-Phe-L-Phe-Gly-benzyl ester) as fF-GOBz.[19]

Although these peptides have been found to be effective in inhibiting vesicle–vesicle fusion and virus–cell fusion involving the sendai virus, these peptides do not inhibit hemagglutinin (HA)-mediated membrane fusion or Ca^{2+} induced fusion, where additional factors or an altogether different mechanism may be involved.[20,21] Stegmann[21] has shown that HA can induce fusion even when the target membrane is fully composed of phosphatidylcholine (PC) which has no tendency to form an H_{II} phase and is in the $L_{\beta'}$ phase. However, there exists a large body of experimental data which clearly suggests the existence of a fusion mechanism involving nonlamellar fusion intermediate structures.[12,13,18]

A molecular-level understanding of peptide/bilayer interactions is crucial to increase our understanding of the fusion inhibition mechanism of these peptides. Moreover, through an understanding of the mechanism of fusion inhibition we should also be able to garner insights into how a peptide might facilitate fusion. How to get this information, though, is unclear because traditional methods (*e.g.*, X-ray crystallography and NMR) used to obtain atomic-level detail are not readily applicable to biomembranes due to their disordered nature in the liquid–crystalline state. Recently, molecular dynamics simulations have been applied to biomembranes in order to obtain molecular-level details of the structure and dynamics of these systems.[22–24] This work is important because this method can provide atomic detail on highly disordered systems like liquid–crystalline

bilayers.[22–24] Thus, computer simulation techniques applied to peptide/lipid systems have the ability to provide structural insights that are difficult to obtain otherwise.

Our current work has been aimed at investigating the effect fusion inhibiting peptides have on the structure and dynamics of *N*-Me-DOPE lipid bilayers using molecular dynamics simulations. Although it is nearly impossible to simulate such events as membrane fusion due to constraints on the system size and time scale, we expect that the effects of the FIPs in the fusion inhibition process will manifest themselves in the structural and dynamical properties of the lipids, which could be understood in terms of a molecular-level mechanism.

Materials and Methods

Force Field. The partial charges were obtained by electrostatic potential (ESP) fitting of *N*-Me-DOPE and Z-D-Phe-L-Phe-Gly (ZfFG) molecules at the STO-3G* level.[25,26] These partial charges are given in Tables 1–3. All hydrogen atoms have been included in the simulations. The force constant and reference bond distance associated with the sp^2 carbons in the C=C bond in the alkyl chains of *N*-Me-DOPE have been taken from the MM2 force field.[27] The nonbond interactions are represented by the all-atom AMBER force field[28] and a cut off distance of 12 Å has been used. Each lipid and FIP has been considered as a single residue, and the nonbond interactions have been calculated using the residue based scheme, so the effective cutoff will be larger than 12 Å.[29]

Solvent Simulations. No direct experimental data on the orientation of the FIPs in the bilayer has been obtained. In order to get some insight into the possible orientations of these peptides in lipid bilayers, we have performed several molecular dynamics simulations on these molecules in different solvent environments. Simulations of both neutral and ionized ZfFG were conducted in water, hexane, and in hexane–water environments. SPC/E water[30] and a united atom hexane model[31] were used in these simulations. The neutral form of ZfFG (heretofore referred to as ZfFG0) was simulated in water, hexane, and hexane–water environments. Two simulations were carried out in the hexane–water environment using a shell of 52 and 116 water molecules around the peptide. The charged form (heretofore referred to as ZfFG⁻) was simulated only in the hexane–water environment with a shell of 119 water molecules around the peptide. A Na^+ was placed in the water shell to maintain the charge neutrality of the total system. In all cases the entire system was energy minimized followed by equilibration which involved slow heating of the system to the final temperature (310 K) over several picoseconds. Subsequently, MD equilibration runs were carried out under constant temperature and constant pressure conditions[32] for 60 ps, which were followed by 120 ps of sampling.

(16) Kelsey, D. R.; Flanagan, T. D.; Young, J.; Yeagle, P. L. Peptide Inhibitors of Enveloped Virus Infection Inhibit Phospholipid Fusion and Sendai Virus Fusion with Phospholipid Vesicles. *J. Biol. Chem.* **1990**, *265*, 12178–12183.

(17) Kelsey, D. R.; Flanagan, T. D.; Young, J.; Yeagle, P. L. Inhibition of Sendai Virus Fusion with Phospholipid Vesicles and Human Erythrocyte Membranes by Hydrophobic Peptides. *Virology* **1991**, *182*, 690–702.

(18) Yeagle, P. L.; Young, J.; Hui, S. W.; Epand, R. M. On the Mechanism of Inhibition of Viral and Vesicle Membrane Fusion by Carbobenzoxy-D-phenylalanyl-L-phenylalanylglycine. *Biochemistry* **1992**, *31*, 3177–3183.
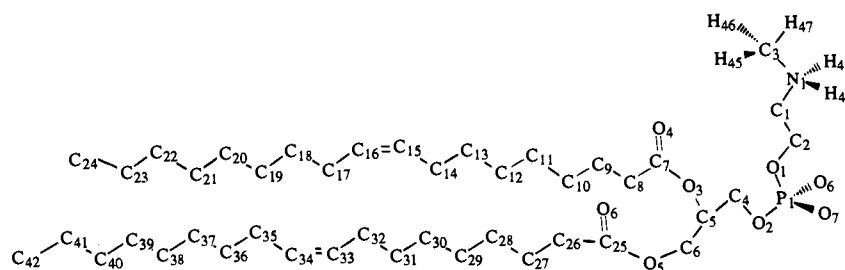
(19) Epand, R. M.; Epand, R. F.; Richardson, C. D.; Yeagle, P. L. Structural Requirements for the Inhibition of Membrane Fusion by Carbobenzoxy-D-Phe-Phe-Gly. *Biochim. Biophys. Acta* **1993**, *1152*, 128–134.

(20) Stegmann, T. Membrane Fusion-Inhibiting Peptides Do Not Inhibit Influenza Virus Fusion or the Ca⁺-induced Fusion of Negatively Charged Vesicles. *J. Biol. Chem.* **1993**, *268*, 26886–26892.

(21) Stegmann, T. Influenza Hemagglutinin-mediated Membrane Fusion Does Not Involve Inverted Phase Lipid Intermediates. *J. Biol. Chem.* **1993**, *268*, 1716–1722.

(22) Pastor, R. W. Molecular Dynamics and Monte Carlo Simulations of Lipid Bilayers. *Curr. Opin. Struct. Biol.* **1994**, *4*, 486–492.

(23) Damodaran, K. V.; Merz, K. M., Jr. Computer Simulation of Lipid Systems. In *Reviews in Computational Chemistry*; Lipkowitz, K. B., Boyd, D. B., Eds.; VCH Publishers: New York, 1994; Vol. 5; pp 269–298.

(24) Stouch, T. R. Lipid Membrane Structure and Dynamics Studied by All-Atom Molecular Dynamics Simulations of Hydrated Phospholipid Bilayers. *Molecular Simulation* **1993**, *102*–106, 335–362.

(25) Besler, B. H.; Merz, Jr., K. M.; Kollman, P. A. Atomic Charges Derived from Semiempirical Methods. *J. Comput. Chem.* **1990**, *11*, 431–439.

(26) Merz, K. M., Jr. Analysis of a Large Database of Electrostatic Potential Derived Atomic Point Charges. *J. Comput. Chem.* **1992**, *13*, 749–767.

(27) Allinger, N. L.; Sprague, J. T. Conformational Analysis. LXXXIV. A Study of the Structures and Energies of Some Alkenes and Cycloalkenes by the Force Field Method. *J. Am. Chem. Soc.* **1972**, *94*, 5734–5747.

(28) Weiner, S. J.; Kollman, P. A.; Case, D. A.; Singh, U. C.; Ghio, C.; Alagona, G.; Profeta, S.; Weiner, P. A New Force Field fo Molecular Mechanical Simulation of Nucleic Acids and Proteins. *J. Am. Chem. Soc.* **1984**, *106*, 765–784.

(29) Alper, H. E.; Bassolino, D.; Stouch, T. R. Computer Simulation of a Phospholipid monolayer-water System: The Influence of Long Range Forces on Water Structure and Dynamics. *J. Chem. Phys.* **1993**, *98*, 9798–9807.

(30) Berendsen, H. J. C.; Grigera, J. R.; Straatsma, T. P. The Missing Term in Effective Pair Potentials. *J. Phys. Chem.* **1987**, *91*, 6289–6271.

(31) Jorgensen, W. L.; Madura, J. D.; Swenson, C. J. Optimized Intermolecular Potential Functions for Liquid Hydrocarbons. *J. Am. Chem. Soc.* **1984**, *106*, 6638–6646.

(32) Berendsen, H. J. C.; Postma, J. P. M.; van Gunsteren, W. F.; DiNola, A. D.; Haak, J. R. Molecular Dynamics with Coupling to an External Bath. *J. Chem. Phys.* **1984**, *81*, 3684–3690.

Table 1. Partial Charges from ESP Fitting of the N-Me-DOPE Molecule[a]

```
                                           H46,,,   H47
                                             \   /
                                        H45► C3
                                             \ N /►H43
                                              |  ►H44
                                              C1
                                       O4     |
                                       ||     C2
   C24  C22   C20   C18   C16=C15  C13  C11  C9  C7   O1
      C23   C21  C19   C17   C14  C12  C10  C8  O3  C4  O6
                                              O6       \  / ►P1◄ O6
      C41   C39   C37   C35      C32   C30   C28   C26-C25   C5  O2  O7
   C42  C40  C38  C36  C34=C33  C31  C29  C27      O5  C6
```

N1	0.1361	O3	−0.6066	C16	−0.0941	O5	−0.4867	C34	−0.1119
C3	−0.2944	C7	0.8346	H16	0.0509	C25	0.8755	H63	0.0538
H45	0.1437	O4	−0.4604	C17	−0.0306	O8	−0.4709	C35	0.0046
H46	0.1437	C8	−0.3641	H17	0.0356	C26	−0.4448	H64	0.0260
H47	0.1437	H1	0.1036	H18	0.0356	H48	0.1174	H65	0.0260
H43	0.2314	H2	0.1036	C18	−0.1120	H49	0.1174	C36	−0.1693
H44	0.2314	C9	−0.0610	H19	0.0518	C27	0.0154	H66	0.0553
C1	−0.1483	H3	0.0354	H20	0.0518	H50	0.0343	H67	0.0553
H41	0.1269	H4	0.0354	C19	0.0094	H51	0.0343	C37	−0.0284
H42	0.1269	C10	0.0279	H21	0.0228	C28	−0.1379	H68	0.0236
C2	0.0889	H5	0.0183	H22	0.0228	H52	0.0539	H69	0.0236
H39	0.0276	H6	0.0183	C20	−0.1133	H53	0.0539	C38	−0.0224
H40	0.0276	C11	−0.0770	H23	0.0389	C29	−0.0040	H70	0.0196
O1	−0.4111	H7	0.0339	H24	0.0389	H54	0.0334	H71	0.0196
P1	0.9640	H8	0.0339	C21	−0.0745	H55	0.0334	C39	−0.0768
O6	−0.6364	C12	−0.0983	H25	0.0334	C30	−0.2127	H72	0.0258
O7	−0.6364	H9	0.0310	H26	0.0334	H56	0.0765	H73	0.0258
O2	−0.4111	H10	0.0310	C22	−0.0867	H57	0.0765	C40	−0.0789
C4	−0.0088	C13	−0.0406	H27	0.0404	C31	0.0168	H74	0.0318
H37	0.0581	H11	0.0293	H28	0.0404	H58	0.0301	H75	0.0318
H38	0.0581	H12	0.0293	C23	0.0831	H59	0.0301	C41	0.1087
C5	0.4598	C14	−0.0306	H29	0.0054	C32	0.0046	H76	0.0001
H36	0.0191	H13	0.0356	H30	0.0054	H60	0.0260	H77	0.0001
C6	0.0008	H14	0.0356	C24	−0.2976	H61	0.0260	C42	−0.3167
H34	0.0618	C15	−0.0941	H31	0.0684	C33	−0.1119	H78	0.0721
H35	0.0618	H15	0.0509	H32	0.0684	H62	0.0538	H79	0.0721
				H33	0.0684			H80	0.0721

[a] Most of the hydrogen atoms associated with the carbon atoms have not been shown for clarity. However, they were included in the simulations.

Atomic coordinates and velocities were collected every 0.030 ps from the pure solvent simulations and one of the hexane−water runs (with 52 water molecules) involving ZfFG0. For the remaining simulations snapshots were examined to determine conformational preferences.

Bilayer Simulations. We have chosen N-methyldioleoylphosphatidylethanolamine (N-Me-DOPE) and Z-D-Phe-L-Phe-Gly (ZfFG) in this investigation because extensive experimental data are available on the fusion behavior of this system in both vesicle−vesicle and vesicle−virus fusion.[16,17] Methylation of the ethanolamine head group results in a small decrease in the critical temperature (T_c) but increases the L_α to H_{II} phase transition temperature (T_H) substantially.[33] With the addition of a single methyl group, T_c decreases by ∼5 K, while T_H increases by ∼55 K. Further, in the case of N-Me-DOPE ($T_c = 258−263$ K, $T_H = 338$ K) isotropic ^{31}P resonances characteristic of nonbilayer structures such as the inverted cubic phase have been observed over a large temperature range (∼308−338 K, the exact range is pH dependent) below T_H.[12,34] A substantial increase in the rate of fusion is also observed in this temperature range.[12,17]
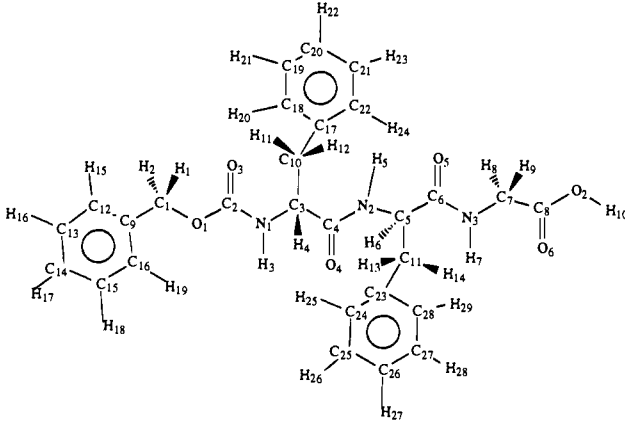
The starting structure for the neat bilayer was made by placing N-Me-DOPE lipids in random orientations in the plane of the bilayer. Our previous simulations of DMPC using this method showed that models built using random starting orientations do not give the collective tilt seen in models built from the crystal structure wherein the alkyl chains are oriented parallel to one another.[35] We have used an area per lipid

of 66 Å² for the neat N-Me-DOPE bilayer, which is the mean value reported by Gruner et al.[34] Each leaflet of the bilayer consisted of 16 lipids, and we have intercalated four ZfFG0 peptides into one of the monolayers of the N-Me-DOPE bilayer model using the structure of the peptide obtained from the solvent simulations (see Results and Discussion section for further details). Since the incorporation of the peptide is expected to cause an increase in the area per lipid, we have used an area per lipid about 10% larger (72.6 Å²) than that used for the neat system. To complete the starting model ∼25 SPC/E water molecules per lipid were added to the head group region of the system. In the beginning of the simulation all the lipid head groups were extended into the solvent region. This geometry was helpful for building the starting models because it avoided repulsive lipid−lipid as well as lipid−peptide nonbonded contacts. After minimization, the lipid head groups and the water molecules were allowed to undergo MD equilibration for several picoseconds. The box dimension along the bilayer normal was allowed to vary under a constant pressure of 1 atm,[32] while the other two directions were held constant (these values were fixed by the area per lipid used). This procedure allowed the head groups to become parallel to the bilayer surface and water molecules to diffuse into the interface region to a small extent, while the bilayer thickness decreased gradually. The total system was then allowed to undergo unrestrained molecular dynamics. During this period the temperature was increased gradually to the target value of 310 K by coupling to a temperature bath.[32] After about 100 ps of equilibration the box dimension along the bilayer normal stabilized. Following the equilibration phase atomic coordinates and velocities were collected every 0.030 ps for 300 ps using constant volume periodic boundary conditions.

(33) Gagne, J.; Stamatatos, L.; Diacovo, T.; Hui, S. W.; Yeagle, P.; Silvius, J. Physical Properties and Surface Interactions of Bilayer Membranes Containing N-Methylated Phosphatidylethanolamine. *Biochemistry* **1985**, *24*, 4400−4408.

(34) Gruner, S. M.; Tate, M. W.; Kirk, G. L.; So, P. T. C.; Turner, D. C.; Keane, D. T.; Tilcock, C. P. S.; Cullis, P. R. X-ray Diffraction Study of the Polymorphic Behavior of N-Methylated Dioleoylphosphatidylethanolamine. *Biochemistry* **1988**, *27*, 2853−2866.

(35) Damodaran, K. V.; Merz, K. M., Jr. A Comparison Between DMPC and DLPE Based Lipid Bilayers. *Biophys. J.* **1994**, *66*, 1076−1087.
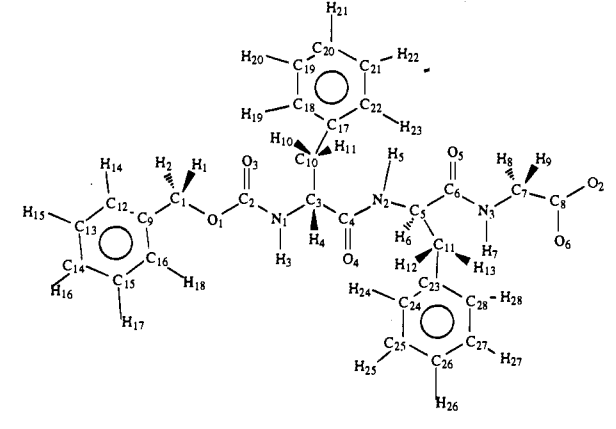
Table 2. Partial Charges from ESP Fitting of the Z-d-Phe-l-Phe-Gly Molecule

C1	−0.1448	N1	−0.8871	N2	−0.4655	N3	−0.5095
H1	0.0879	H3	0.3034	H5	0.2580	H7	0.3315
H2	0.0879	C3	0.5345	C5	−0.1986	C7	−0.4550
C9	0.1805	H4	−0.0427	H6	0.1249	H8	0.1632
C12	−0.1434	C10	−0.3536	C11	−0.2945	H9	0.1632
H15	0.0937	H11	0.0750	H13	0.0952	C8	0.8300
C13	−0.0606	H12	0.0750	H14	0.0952	O6	−0.4631
H16	0.0647	C17	0.2433	C23	0.2110	O2	−0.5630
C14	−0.0480	C18	−0.1583	C24	−0.1363	H10	0.3506
H17	0.0583	H20	0.0817	H25	0.0645		
C15	−0.0606	C19	−0.0626	C25	−0.0463		
H18	0.0647	H21	0.0680	H26	0.0643		
C16	−0.1434	C20	−0.0663	C26	−0.0771		
H19	0.0937	H22	0.0646	C27	0.0635		
O1	−0.3521	C21	−0.0626	C27	−0.0463		
C2	0.9870	H23	0.0680	H28	0.0643		
O3	−0.5058	C22	−0.1583	C28	−0.1363		
		H24	0.0817	H29	0.0645		
		C4	0.4000	C6	0.7047		
		O4	−0.3599	O5	−0.3606		

Table 3. Partial Charges from ESP Fitting of the [Z-d-Phe-l-Phe-Gly]⁻ Molecule

C1	−0.1299	N1	−0.8939	N2	−0.5501	N3	−0.6202
H1	0.0831	H3	0.3073	H5	0.2579	H7	0.3240
H2	0.0831	C3	0.5523	C5	−0.0437	C7	−0.1962
C9	0.1710	H4	−0.0497	H6	0.0767	H8	0.0586
C12	−0.1386	C10	−0.3601	C11	−0.2743	H9	0.0586
H14	0.0941	H10	0.0719	H12	0.0781	C8	0.6132
C13	−0.0623	H11	0.0719	H13	0.0781	O6	−0.6794
H15	0.0628	C17	0.2443	C23	0.2062	O2	−0.6794
C14	−0.0500	C18	−0.1582	C24	−0.1429		
H16	0.0551	H19	0.0805	H24	0.0786		
C15	−0.0623	C19	−0.0618	C25	−0.0460		
H17	0.0628	H20	0.0676	H25	0.0605		
C16	−0.1386	C20	−0.0661	C26	−0.0900		
H18	0.0941	H21	0.0617	H26	0.0557		
O1	−0.3470	C21	−0.0618	C27	−0.0460		
C2	0.9812	H22	0.0676	H27	0.0605		
O3	−0.5099	C22	−0.1582	C28	−0.1429		
		H23	0.0805	H28	0.0786		
		C4	0.4187	C6	0.6766		
		O4	−0.3463	O5	−0.3677		

The final configuration from the ZfFG0:*N*-Me-DOPE run was used to generate the starting structure for ZfFG⁻:*N*-Me-DOPE. We examined both ZfFG0 and ZfFG⁻ in order to separately evaluate the role hydrophobic interactions play relative to strong electrostatic interactions. In terms of the experimental conditions used to examine these peptides we note that the peptide is expected to be ionized. To neutralize the system four water molecules in the solvent region were replaced with Na⁺ ions. This system was further equilibrated under constant pressure as described above, for 100 ps before collecting a trajectory for 300 ps under constant volume periodic boundary conditions. By placement of the peptides onto only one leaflet of the bilayer one might imagine that the bilayer might be driven into a wedge shape and not the rectangular shape used with periodic boundary conditions. We feel that this effect is not important because the intercalated peptides eject water molecules in the headgroup region of the biomembrane, thus, releasing enough free volume for the peptides to occupy. The leaflet without the peptides retain water molecules in the headgroup of the biomembrane thereby equalizing the free volume occupied by the two leaflets. Furthermore, FIPs carry out their function by only intercalating into one leaflet of a bilayer, so the model we have used is representative of the experimental situation. However, in order to computationally test this question we have run a shorter trajectory (~100 ps equilibration + 80 ps sampling) in which four ZfFG0 peptides were intercalated on both monolayers of the bilayer.

Results and Discussion

Peptide Conformation and Environment in Solvent Simulations. The peptide conformations for ZfFG0 from the pure solvent (water, hexane) runs have been compared to those obtained from the hexane/water runs using Ramachandran plots and visual analysis. The ϕ-ψ maps for the three trajectories

are given in Figure 1. It is clear from this figure that the peptide in the hexane−water simulation has explored more regions of conformational space than the pure solvent simulations. The time dependence of the ϕ and ψ torsion angles also showed that the lifetime for the peptide in a certain conformational region is about 100 ps (data not shown). Thus, the low concentration of the data points for example, in the (−60,−60) region in the ϕ-ψ map for L-Phe is due to the finite length of the simulation. The observed conformational flexibility may be important for these peptides in partitioning into the lipid bilayers. For example, the high conformational flexibility, while potentially allowing the peptides to adopt more readily to the bilayer environment, ultimately will result in an entropic penalty upon final attachment to the bilayer surface. This suggests that rigid molecules that can form the bioactive conformation may be more effective antifusogenic compounds.

Graphical visualization of snapshots of the peptide in the mixed solvent environment provided interesting insights about the peptide/solvent interactions, which might have implications on the placement of these peptides in lipid bilayers. Typical snap shots from the hexane−water run of ZfFG0 and ZfFG⁻ given in Figure 2a,b show that all the water molecules have accumulated on one side of the peptide such that peptide/water hydrogen bonds could be retained. Furthermore, favorable hydrophobic contacts are also generated by placing the phenyl groups into hexane. This behavior was also observed with the negatively charged peptide ZfFG⁻.

The orientation of the peptide from the water/hexane simulations suggested that docking the peptide into the bilayer−water interface with the plane of the peptide backbone parallel to the
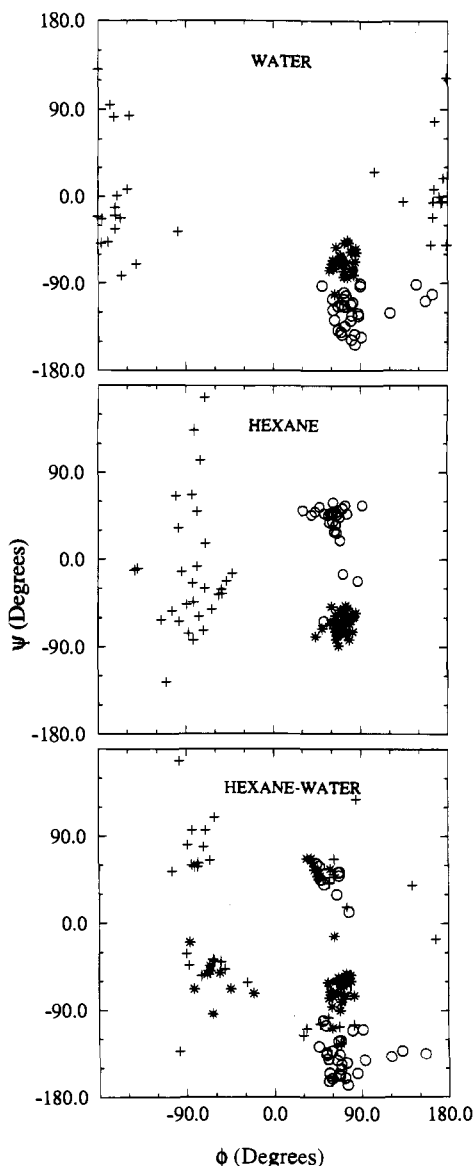
Figure 1. Ramachandran plots for ZfFG0 from the solvent simulations. Labels are as follows: (O) D-Phe, (*) L-Phe, and (+) Gly. The data points were collected every 3 ps from 120 ps trajectories.
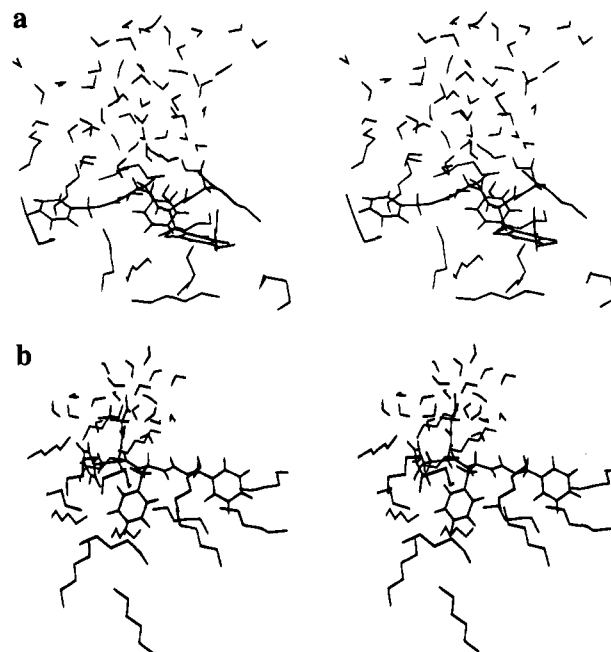

Figure 2. Stereo plot showing the water—hexane environment of (a) ZfFG0 and (b) ZfFG⁻ in the mixed hexane/water simulations.

backbone of the lipids, while the charged N-terminal region is anchored in the interface.

Peptide Conformation in the Bilayer. The conformation of the peptides in the bilayer were also probed by calculating ϕ-ψ maps which are presented in Figure 3 for the neutral and charged peptides. In Figure 4 we also give stereo snapshots of the observed conformations of FIPs in the bilayer. The initial bilayer/peptide model had all four peptides in the same conformation, and the lipid environments were chosen to be as similar as possible. Note, however, that identical lipid environments could not be constructed due to the random orientations of the lipids in the plane of the bilayer. Not unexpectedly, we observe that the peptides have reduced conformational freedom in the bilayer relative to the solvent environment, but this lack of sampling has been allayed to some extent by having several peptides in the model. In the case of ZfFG0 three of the four peptides in the model have very similar conformations (peptides 1, 3, and 4). Peptide 2, on the other hand, has adopted a different conformation as revealed by the ϕ-ψ plots in Figure 3. In the charged system which is more representative of the experimental case, a large fraction of the conformations are in a different ϕ-ψ region compared to the neutral system. However, we note that all the ϕ-ψ regions observed in the bilayer simulations have been sampled by the peptides in the mixed solvent (hexane/water) environment. Visual inspection of the bilayer/peptide system and density profiles (see below) also revealed that the neutral peptides sampled different orientations with respect to the extent of penetration of the phenyl rings into the hydrocarbon region, while in the charged case, most of the phenyl rings were fully inserted. The reason for this observation probably has to do with the enhanced ability of the charged C-terminal carboxylate to anchor the FIPs into the headgroup region of the bilayer. Hence, while hydrophobic interactions certainly play a role in favoring the intercalation of the peptide into the bilayer, it is clearly an interplay between the charge and hydrophobic interactions that results in a strong interaction between the peptides and the lipids contained within the bilayer.

bilayer surface (as opposed to an orientation perpendicular to the bilayer surface) would be a favorable orientation. The peptides placed in this manner have the hydrophobic phenyl rings intercalated into the membrane interior (roughly at the carbonyl region), while the C-terminal region of the peptide is in the interfacial region of the bilayer. Naively, therefore, one can view these peptides as having amphipathic characteristics where the "headgroup" is the C-terminal carboxyl group, while the "alkyl region", which is suitably removed from the headgroup by a linker group, consists of the phenyl rings. The starting configuration we have selected to start our simulations is further justified from experimental observations. For example, Jacobs and White[36] on the basis of neutron diffraction data have shown that the peptide Ala-Trp-Ala-O-tert-butyl places the hydrophobic indole ring into the interior of the membrane, while the backbone resides in the interfacial region. Brown and Huestis[37] from NMR studies on Ala-Phe-Ala-O-tert-butyl have determined that the phenyl ring resides near the

(36) Jacobs, R. E.; White, S. H. The Nature of the Hydrophobic Binding of Small Peptides at the Bilayer Interface: Implications for the Insertion of Transbilayer Helices. *Biochemistry* **1989**, *28*, 3421–3437.

(37) Brown, J. W.; Huestis, W. H. Structure and Orientation of a Bilayer-Bound Model Tripeptide. A ¹H NMR Study. *J. Phys. Chem.* **1993**, *97*, 2967–2973.
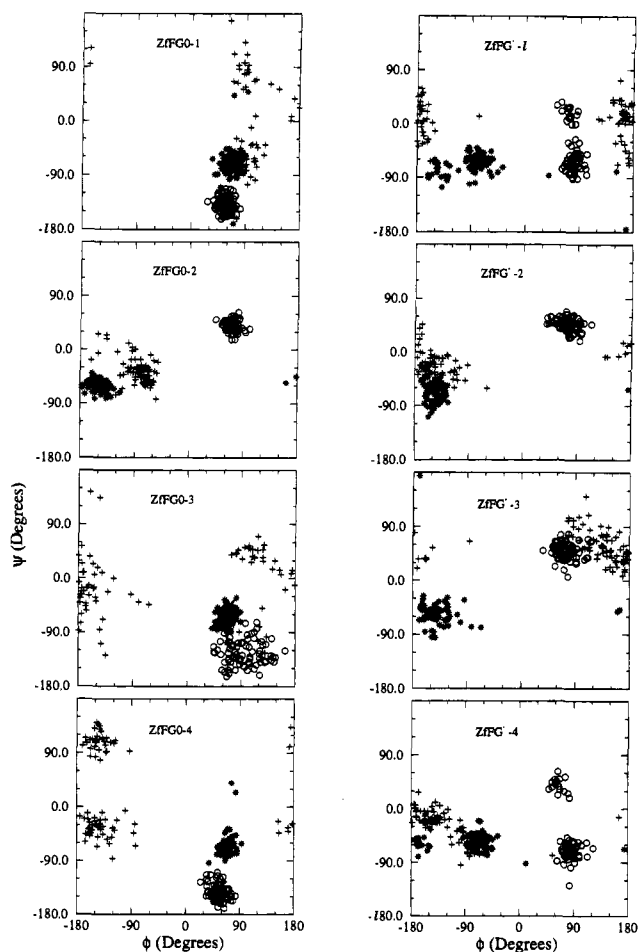
Figure 3. Ramachandran plots for ZfFG⁻ and ZfFGO from the bilayer simulations. Data points were collected every 6 ps from a 300 ps trajectory. Symbols for residues are the same as those used in Figure 1.

Lipid Conformation And Dynamics Order Parameters

The molecular long axis order parameters were calculated for the neat *N*-Me-DOPE and *N*-Me-DOPE:FIP systems using eq 1

$$S_n = F\left(\frac{1}{2}\right)\langle(3\cos^2\beta_n - 1)\rangle \tag{1}$$

where β_n is the angle between the bilayer normal and the vector joining carbons $n - 1$ and $n + 1$ in the alkyl chains.[38] Assuming axial symmetry, the NMR order parameters can be obtained from the S_ns by multiplying by 0.50.[39] The profiles have been calculated for the two leaflets of the bilayer separately and have been averaged over the 300ps MD trajectory.

The order parameter profiles for the leaflet containing the peptides (both neutral and charged models) are shown in Figure 5a. We have also included in this figure the profile from the "neat" *N*-Me-DOPE simulation. It is clear from this figure that the leaflet with the FIPs show larger order parameters (*i.e.*, an increase in ordering), particularly in the upper part of the alkyl region. This observation is likely due to the additional van der Waals interactions between the alkyl chains of the lipids and the phenyl rings of the FIPs which penetrate into the upper

(38) Pastor, R. W.; Venable, R. M.; Karplus, M. Brownian Dynamics Simulation of a Lipid Chain in a Membrane Bilayer. *J. Chem. Phys.* **1988**, *89*, 1112–1127.

(39) Seelig, J. Deuterium Magnetic Resonance: Theory and Application to Lipid Membrances. *Quarterly Reviews of Biophysics* **1977**, *10*, 353–418.
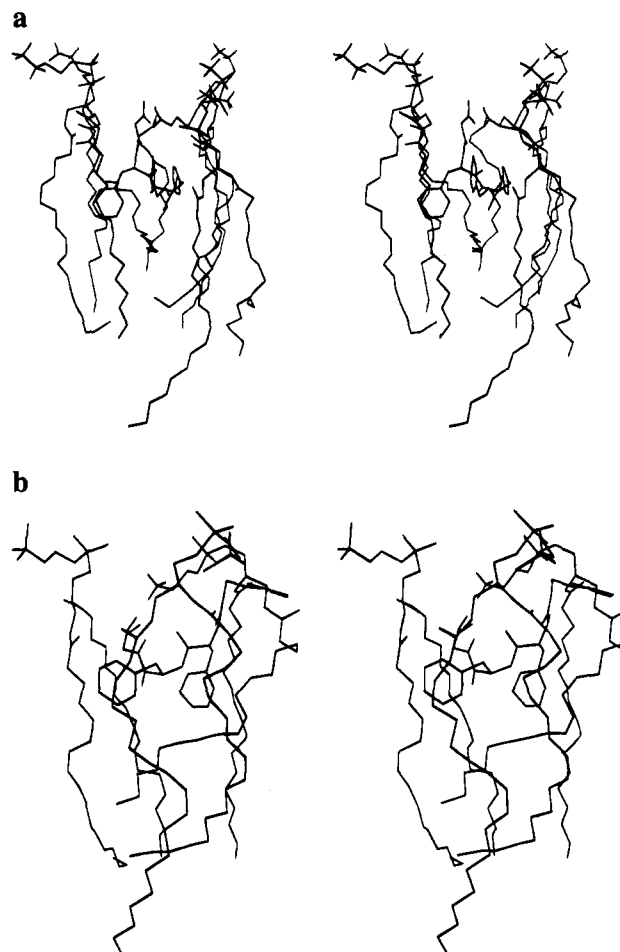

Figure 4. Stereo plots of snap shots from bilayer/peptide simulations. (a) ZfFG⁻ and (b) ZfFGO.

portion of the hydrocarbon region of the bilayer. We also observe that the order parameters are higher in the charged model due to the insertion of a larger fraction of the phenyl rings. Hence, enhanced partitioning of the phenyl rings into the bilayer results in a further reduction in the mobility of the alkyl chains in this region. In the interior of the alkyl region (carbon atoms 10–17) the order parameters for the leaflet with the peptides are lower than that observed for the neat simulation. This reduction is due to two effects. The first involves the larger area per lipid used in the simulations that contained the peptides. This automatically ensures that the order parameters for the leaflets with the peptides will be lower than the "neat" leaflet. The second effect arises from the presence of the peptide, which may cause an increase or decrease in the order parameters in this region.

In order to determine if the peptide is ordering or disordering the lower alkyl region we examined order parameters from a neat simulation in which the area per lipid was increased to that used in the bilayer that contained the FIP. The expanded area per lipid "neat" simulation started from the original neat simulation and covered 100 ps of equilibration and 100 ps of sampling. The results of these simulations are given in Figure 5b. Not unexpectedly, we see that the expanded area per lipid bilayer does have a lower order parameter profile than does the original neat simulation. It is also clear that the ordering effect at the bilayer interface for the leaflet containing the peptide is the result of the intercalation of the peptide into the bilayer. Note also that the leaflet that does not contain the peptide in
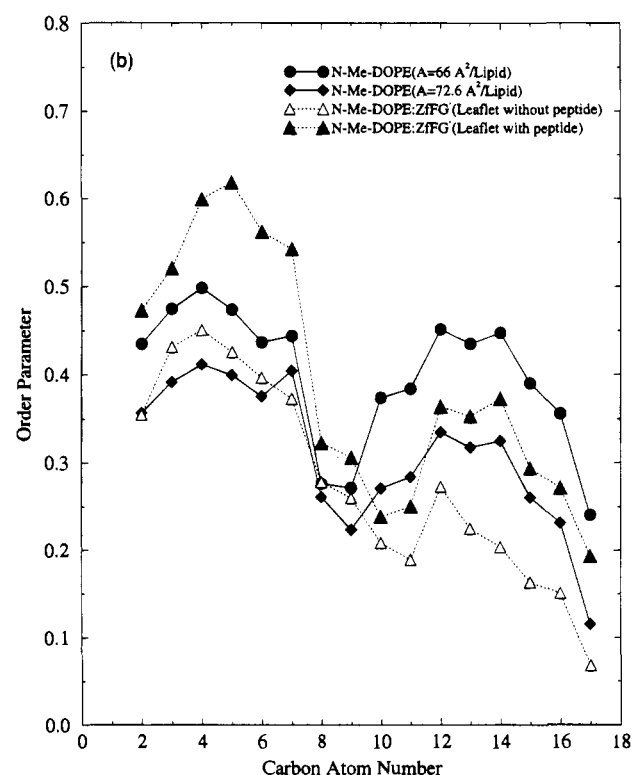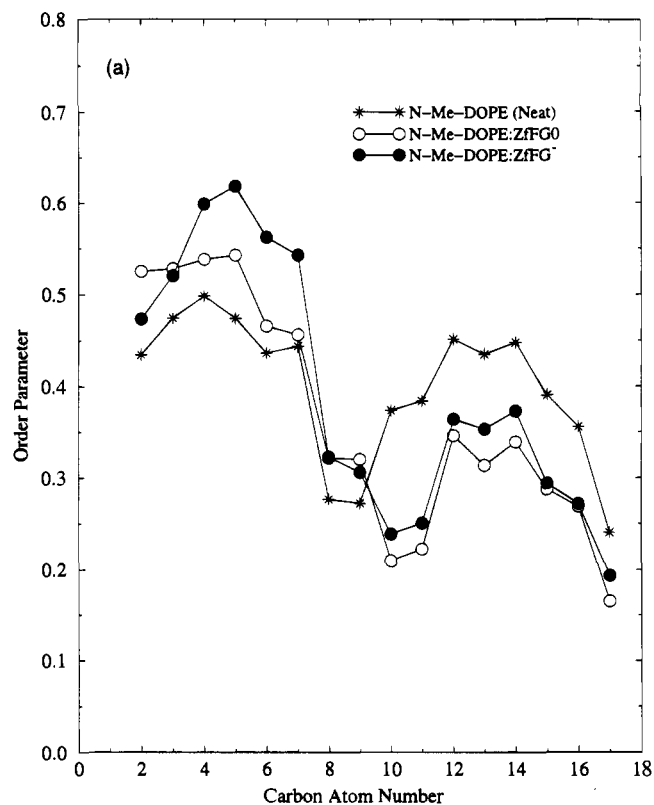
Figure 5. Order parameter profiles for the neat bilayer and the bilayer–peptide systems. (a) Comparison of the order parameters for the leaflets with the peptides to a neat bilayer simulation. (b) Comparison of order parameters for the leaflets with and without peptides to an expanded bilayer simulation.
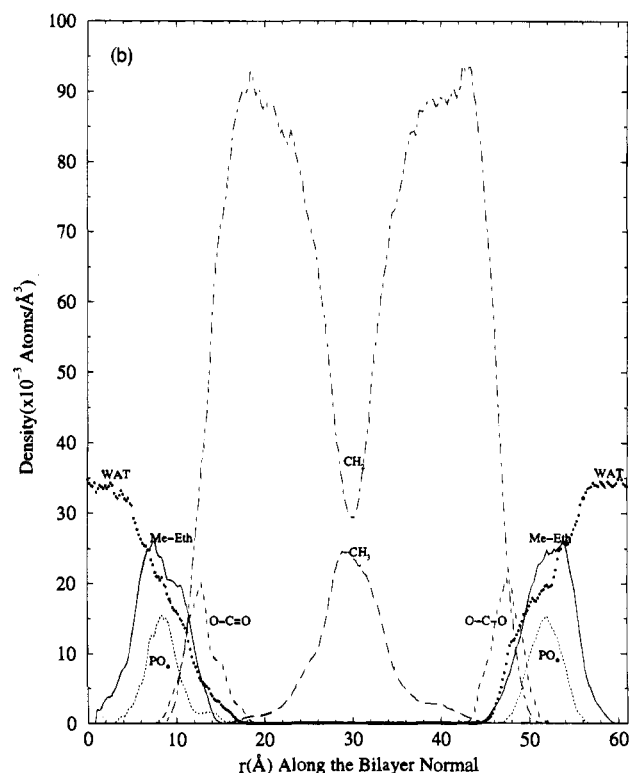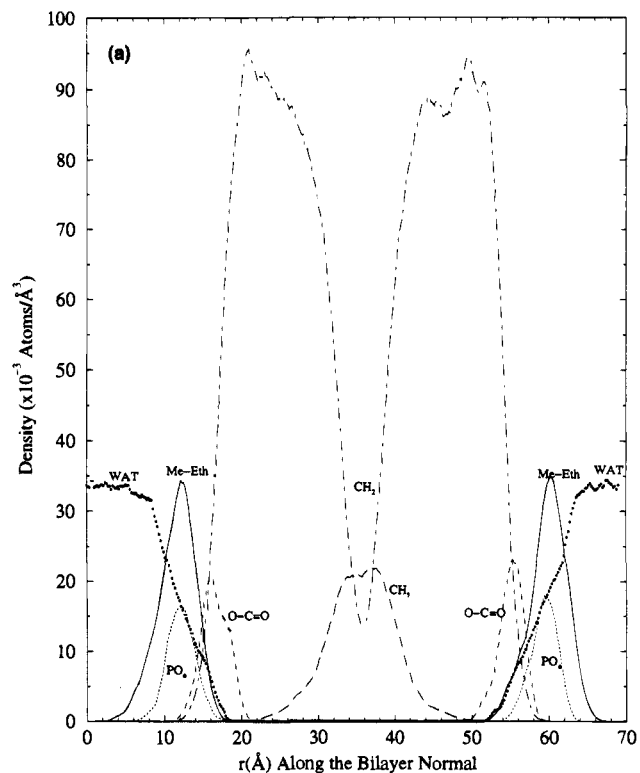
Figure 6. (a) Atomic density profiles along the bilayer normal for the water and lipid regions of the neat N-Me-DOPE bilayer. (b) Atomic density profiles along the bilayer normal for the water and lipid regions of the expanded neat N-Me-DOPE bilayer.

the ZfFG⁻ (open triangles in Figure 5b) simulation and the expanded bilayer model has similar order parameters for carbon atoms 2–8. However, in the interior alkyl region for this leaflet it appears that the enhanced disorder present is due to communication with the leaflet that contains the peptide. This same

effect has been observed in an earlier simulation from our laboratory on the "white" peptide Ala-Phe-Ala-O-tert-butyl intercalated into a DMPC bilayer.[40] We believe the origin of the transmission of a perturbation of a bilayer from one leaflet to another results from the loss of interleaflet alkyl contacts.

(40) Damodaran, K. V.; Merz, K. M., Jr.; Gaber, B. P. Interaction of Small Peptides with Lipid Bilayers. Submitted to *Biophys. J.*
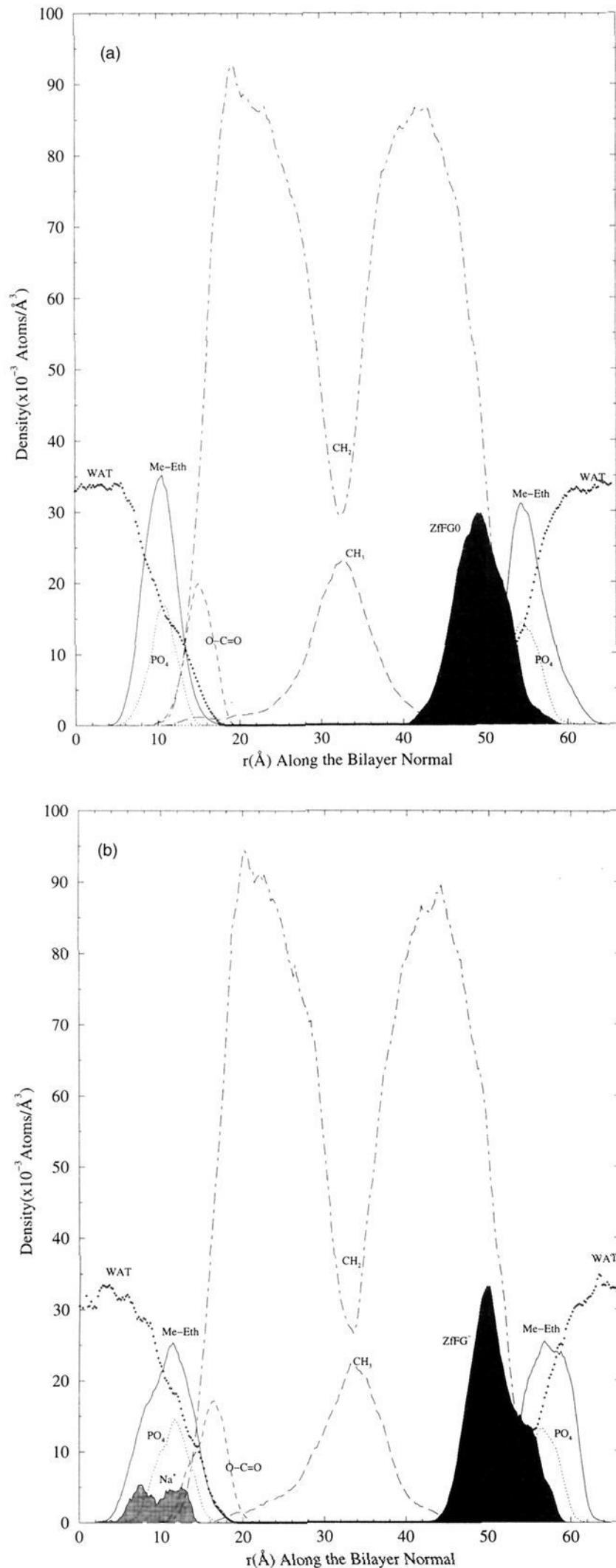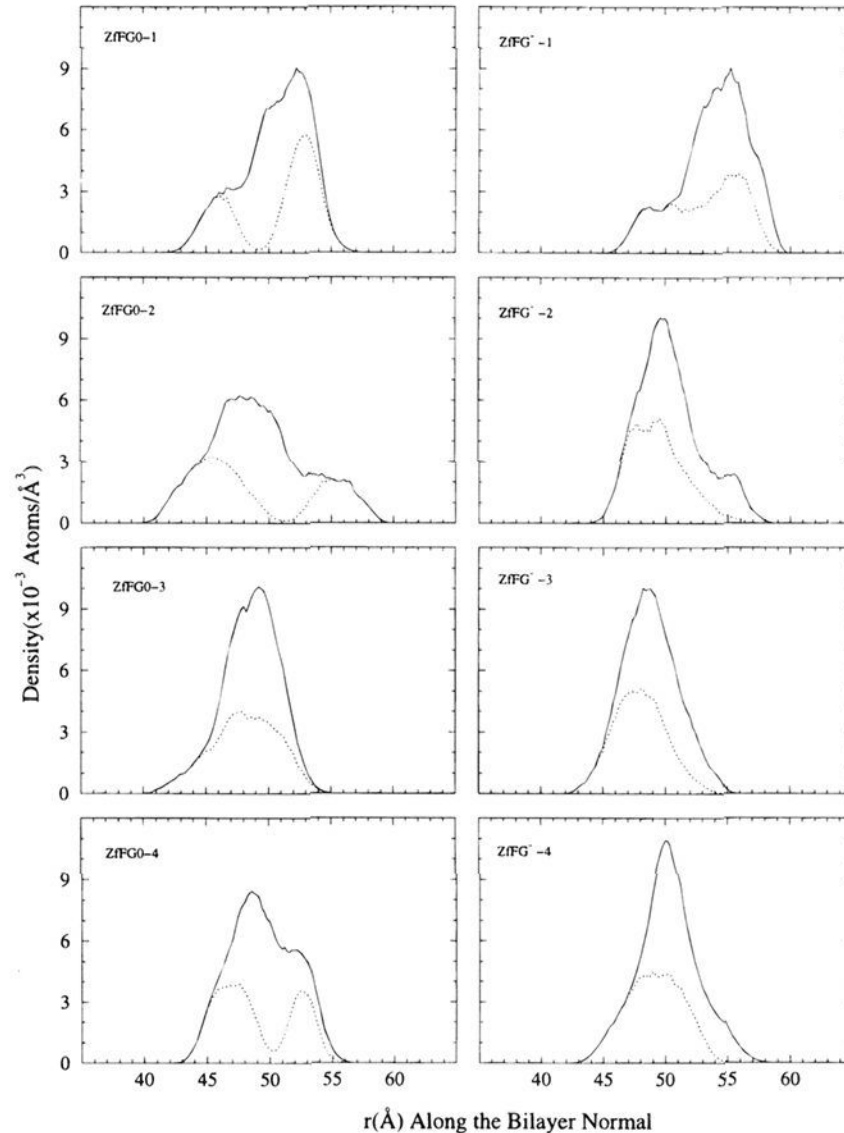
Figure 8. Total (solid lines) and side chain (dotted lines) atomic probability distributions for the peptides along the bilayer normal. The bilayer center is on the low r side (below ~45 Å) and solvent/head group region is on the high r side (~50 Å and above) in these plots.

However, when we compare the order parameters for the expanded bilayer simulation to those from the leaflet with the peptide, we find that even in the interior alkyl region there is a slight increase in the value of the order parameters. Hence, the peptides appear to have an ordering effect on almost the entire alkyl region, but this ordering is most pronounced at the interface.

We would like to view the behavior of the order parameters as the manifestation of a plausible molecular mechanism for fusion inhibition. The increased order parameters show that the additional van der Waals interaction between the peptide side chains and the lipid alkyl region renders the bilayer gel-like instead of driving it toward the H_{II} phase giving rise to the formation of fusion intermediates. Furthermore, models with the neutral and negatively charged FIPS show that the function of these peptides is brought about primarily through hydrophobic interactions with electrostatic interactions having an indirect role. Thus, the propeller-like structure of the side chains in these peptides allows them to intercalate between lipid chains without causing bilayer disruption, while the charged C-terminus on the glycine can extend itself into the head group region to form hydrogen bonding interactions.

Density Profiles. The density profiles for the lipid molecules, FIPs, and water molecules along the bilayer normal have been calculated over the MD trajectories. These distributions are shown in Figures 6–8. The bilayer thicknesses, as estimated by the peak-to-peak distance between N-methylethanolamine density distributions, are ~48.2 Å for the unexpanded neat system, ~44 Å for the expanded neat system, ~43.8 Å for the neutral FIP model, and ~45.4 Å for the charged FIP model. X-ray diffraction studies by Gruner et al.[34] have determined the neat bilayer thickness to be 39 ± 5 Å. Thus, compared to the
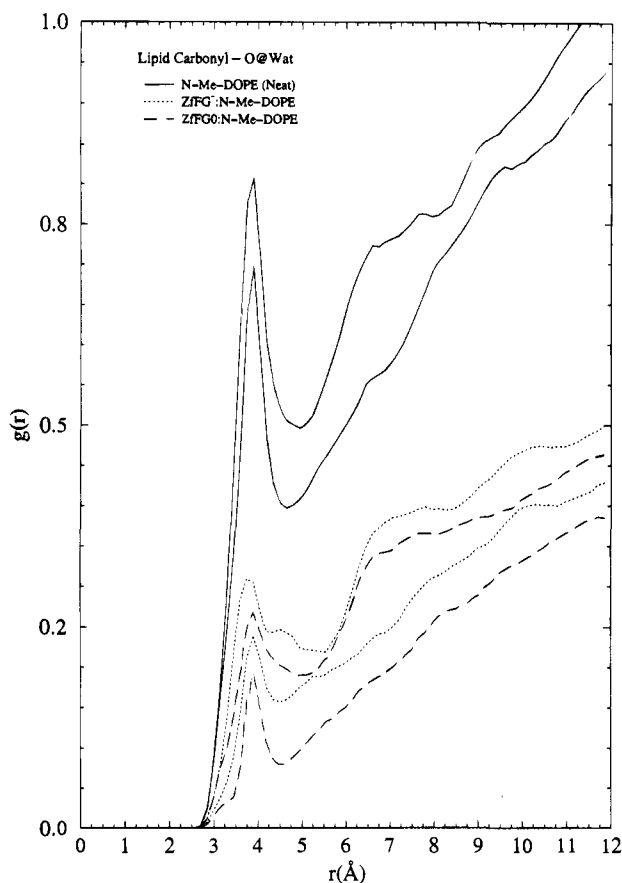

Figure 7. (a) Atomic density profile along the bilayer normal for the peptide, lipid, and water regions from the N-Me-DOPE:ZfFGO simulation. (b) Atomic density profile along the bilayer normal for the peptide, lipid, and water regions from the N-Me-DOPE:ZfFG⁻ simulation. In this figure the counterion (Na⁺) distribution has been amplified by a factor of 10 to have visible intensity.

For example, the leaflet containing the peptides responds to their presence by forming "pockets" around the peptides which results in reduced interleaflet contacts. We also note that in the lower alkyl region the order parameters in the monolayer with the peptide are lower than those in the unexpanded neat profile.

Figure 9. Pair distribution functions for water from the lipid carbonyls. Carbonyls on the Sn-1 and Sn-2 positions are shown independently.

Figure 10. Pair distribution functions of water from the peptide C-termini. The top figure is for the charge peptide $ZfFG^-$ simulation, and the lower figure is for the neutral peptide ZfFGO simulation.

experimental data, the bilayer thickness for the neat system (see Figure 6) is somewhat larger and as a result slightly more ordered. The smaller dimension for the bilayer with the peptides could partially be due to increased disorder in the alkyl chains caused by the larger area per lipid used in the model.

The FIPs' distribution overlaps partially with those of the lipid head groups, glycerol backbone and alkyl chains as shown in Figure 7a,b. The neutral peptides showed considerable "disorder" among themselves with respect to their orientations and the extent of penetration into the bilayer as shown by the density profiles for the phenylalanyl rings shown in Figure 8. For this system only one peptide (ZfFG0-3) had all the three rings inserted into the alkyl chain region. Two peptides had two rings into the alkyl chain region and one in the head group region, and the fourth peptide had one ring in the alkyl chain region and two rings in the head group region. The charged peptides were much more ordered in this respect. Three of the four peptides had all three rings inserted into the hydrocarbon region while one (ZfFG$^-$-1) had one ring partially exposed to the head group and solvent region. The four sodium ions used as counterions in the *N*-Me-DOPE:ZfFG$^-$ runs were initially placed deep into the aqueous region. During the course of the simulation, these ions drifted closer to the monolayer without the peptides and formed a number of indirect interactions with lipid phosphate groups through their respective hydration shells.

We also note that the presence of the peptides give rise to a slight decrease in the extent of water penetration. Given the largely hydrophobic nature of these peptides, this observation is not unexpected. This can be best seen from the pair distribution functions (pdfs) given in Figures 9 and 10 for water—carbonyl carbon and water—peptide—C-termini interactions. From Figure 9 we can see that the neat pdfs are greater in intensity than the pdfs for the leaflets containing peptides. It
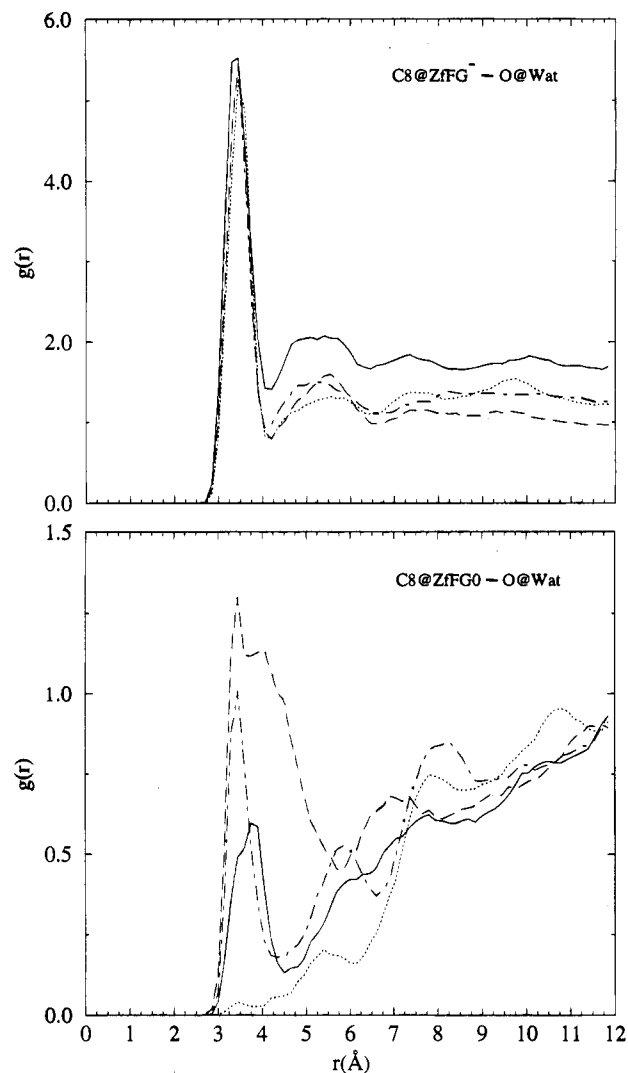
is also interesting to note that the pdfs arising from water—lipid carbonyl interactions are of higher intensity for the charged system than for the neutral system. This likely arises because the charged C-termini structures water molecules around the bilayer/water interface more so than the neutral C-termini. Figure 10 clearly support this conclusion because the charged C-terminal group has greater intensity than does the uncharged. Overall, though, it is clear that the leaflets containing peptide have reduced hydration at the bilayer/water interface. This observation combined with the order parameter data strongly suggests that the FIPs force the leaflet containing them to become more gel-like even at a temperature where the liquid crystalline phase is normally observed.

In these simulations the peptides were placed only on one side of the bilayer which is consistent with the way in which these peptides carry out their fusion inhibiting function. Using this model did not give rise to any anomalous behavior in terms of the calculated observables (*e.g.*, order parameters, *etc.*). This was further confirmed by a short simulation (100 ps equilibration and 150 ps sampling) in which neutral peptides (ZfFG0) were placed on both sides of the bilayer. This model gave order parameter profiles from both monolayers closely resembling the one from the original ZfFG0:*N*-Me-DOPE system (data not shown). This behavior is not unexpected since the free volume occupied by the peptides would have been occupied by water
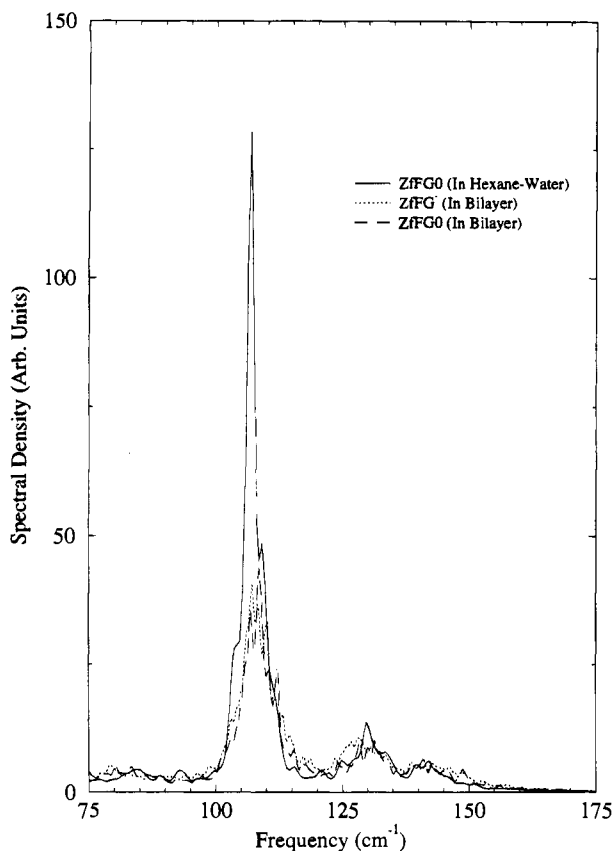
Figure 11. Spectral density plots for the peptide motion from the solvent (hexane/water) and bilayer simulation. The average of spectral densities for the four peptides in the bilayer is shown.

Figure 12. Spectral density plots for the head group (top) and alkyl chain (bottom) dynamics from the neat N-Me-DOPE-Me and N-Me-DOPE:FIP simulations.

molecules in a neat bilayer model. Thus, while the peptides do occupy free volume in the leaflet with the peptides, this same free volume is occupied by water in the leaflet without peptides. This offsets any density differences that might arise in the interfacial region.

Peptide and Lipid Dynamics. The dynamics of the peptide in the bilayer has been compared with that from the solvent runs (hexane/water) using the spectral density plots given in Figure 11. The spectral peak positions have not been shifted significantly from the positions observed in the hexane/water runs in the bilayer simulations. However, the spectral lines in the bilayer have higher full width at half maximum (FWHM) than do the solvent runs. This is not unexpected since the lipid environment is more restrictive compared to the solvent environment which results in an increase in the line widths.

The short time lipid dynamics has also not been significantly affected by the presence of the peptides. This is consistent with the results obtained for the Ala-Phe-Ala-*O-tert*-butyl peptide interacting with a DMPC based bilayer.[40] This observation is clear from the head group and alkyl chain spectral densities given in Figure 12. In the uncharged state (ZfFG0) the peptide—lipid interactions are predominantly van der Waals in nature which only affects lipid groups near the peptide (*e.g.*, the glycerol backbone and the alkyl chain carbon atoms near the carbonyl end of the lipid molecules), while the spectral density peaks have major contributions from carbon atoms far away from these regions. In the case of charged peptides strong electrostatic interactions between the peptide C-termini and lipid phosphate groups are present, which are mediated through water molecules. Since the phosphate groups are relatively immobile, these interactions also do not appear to have a strong effect the lipid head group dynamics. Overall, though these peptides do not appear to have a dramatic effect on the short time scale
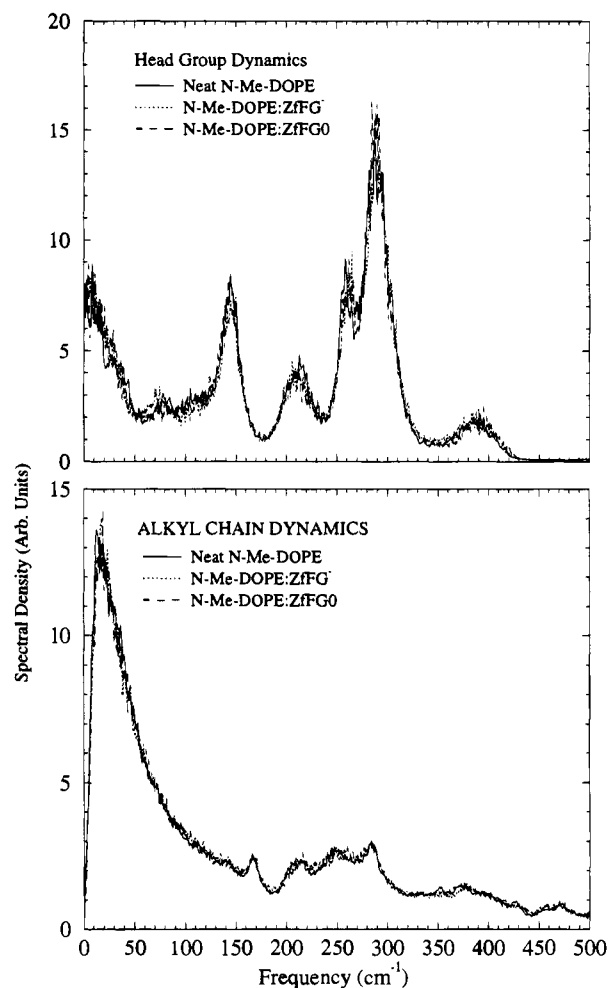
dynamics of the lipid molecules themselves. However, the presence of the peptides do affect the alkyl chain packing which results in the observed increase in order parameters.

Conclusions

Very little is known from experimental investigations about the mechanism of fusion inhibition by these peptides at the molecular level. Isotropic resonances have been observed in ^{31}P NMR experiments of N-Me-DOPE and N-Me-DOPE/DOPC systems in a temperature range below the L_α—H_{II} phase transition temperature, where increased rate of fusion has also been observed.[12] This lends support to the importance of nonlamellar phase preferring lipids in fusion. Electron microscopic studies have shown that the fusion inhibiting peptides can suppress the formation of small unilamellar vesicles and give rise to the formation of large sheet-like structures.[18]

However, structural data about the orientation of the peptides in the bilayer—water interface and the physical parameters of the bilayer—peptide complex are lacking. In this context we have performed bilayer/peptide simulations using plausible models, for which some preliminary insight was obtained from simulations in different solvent environments. The insertion of the peptide side chains into the hydrocarbon regions give rise to increased order in the alkyl chains region, rendering it gel-like. Thus, our simulations show that these peptides are capable of suppressing the formation of structures related to the H_{II} phase, which are potential fusion intermediates.

The apparent contrast observed in the activity of ZfFG and fFGOBz in the fusion of *N*-Me-DOPE vesicles is interesting.[19] While ZfFG, which has a blocked N-terminus and a negatively charged C-terminus, is an efficient fusion suppressant, fFGOBz, on the other hand, which has a charged N-terminus and blocked C-terminus, enhances fusion. This is probably due to the charged N-terminus of D-Phe being very close to its hydrophobic side chain which makes it difficult for the peptide to insert into the bilayer such that its N-terminus is exposed to the head group region while the Phe rings are inserted between the alkyl chains. In ZfFG, the unblocked C-terminus is on Gly, which extends into the head group region, while the Phe rings penetrate into the bilayer interior.

It must also by recognized that the modeling strategy adopted here *i.e.*, MD simulations with cubic periodic boundary conditions, has inherent limitations. First of all, computational resource limitations restrict the model size and more importantly the time scale to which one can carry out these simulations. Another limitation is the use of cubic periodic boundary conditions which makes formation of noncubic structures difficult. Thus, if one has to simulate the formation of the hexagonal phase from the bilayer phase, one has to use different periodic boundary conditions in different regions of the trajectory. In the present work we have looked at properties which might act as indicators of a molecular level mechanism of fusion inhibition by these peptides.

In summary, since it is virtually impossible to simulate the partitioning of fusion inhibiting peptides into the bilayer, the present work has been done in the reverse sequence of events, *i.e.*, start with the peptides in an assumed geometry in the bilayer and allow the system to undergo dynamics. In a real experimental situation, our results suggest that the insertion of FIPs will result in (1) partial exclusion of interfacial waters and (2) increased order in the alkyl chains which may arise from additional van der Waals interactions with the phenylalanyl rings. Our simulations also suggest that ZfFG can adopt an amphipathic structure in many ways similar to the lipid molecules themselves. In this sense the C-termini of ZfFG is the polar headgroup region of ZfFG, while the phenyl rings are the hydrophobic "tails" of the peptides. This observation suggests that other molecules that have antifusogenic properties could be produced if attention is paid to ensuring compatibility between the antifusogen and the lipid molecules that constitute the bilayer. Finally, we conclude that these peptides carry out their function by stabilizing the bilayer phase with respect to nonbilayer phases that may be involved in the fusion process.